

# P-spline smoothed functional ICA of EEG data

Marc Vidal<sup>1,2†‡\*</sup>, Mattia Rosso<sup>2‡</sup>, Ana M. Aguilera<sup>1†</sup>

\*For correspondence:

marc.vidalbadida@ugent.be (M.V.);  
aaguiler@ugr.es (A.M.A.)

Present address: <sup>†</sup> Department of Statistics and O.R., Granada 18071, Spain; <sup>‡</sup>Department of Musicology, IPEM, Gent 9000, Belgium

**Abstract** We propose a novel functional data framework for artifact extraction and removal to estimate brain electrical activity sources from EEG signals. Our methodology is derived on the basis of event related potential (ERP) analysis, and motivated by mapping adverse artifactual events caused by body movements and physiological activity originated outside the brain. A functional independent component analysis (FICA) based on the use of fourth moments is conducted on the principal component expansion in terms of B-spline basis functions. We extend this model setup by introducing a discrete roughness penalty in the orthonormality constraint of the functional principal component decomposition to later compute estimates of FICA. Compared to other ICA algorithms, our method combines a regularization mechanism stemmed from the principal eigendirections with a discrete penalization given by the  $d$ -order difference operator. In this regard, it allows to naturally control high-frequency remnants of neural origin overlapping latent artifactual eigenfunctions and thus to preserve this persistent activity at artifact extraction level. Furthermore, we introduce a new cross-validation method for the selection of the penalization parameter which uses shrinkage to asses the performance of the estimators for functional representations with larger basis dimension and excess of roughness. This method is used in combination with a kurtosis measure in order to provide the optimal number of independent components. The FICA model is illustrated at functional and longitudinal dimensions by an example on real EEG data where a subject willingly performs arm gestures and stereotyped physiological artifacts. Our method can be relevant in neurocognitive research and related fields, particularly in situations where movement can bias the estimation of brain potentials.

**Keywords:** Electroencephalography; Fourth order blind identification; Functional data analysis; Functional independent component analysis; Karhunen-Loëve expansion; Source separation

## 1 Introduction

Human body is a complex self-regulatory system. As a result of physiological activity, some particular organs and individual cells undergo changes in electrical potentials generating a bioelectrical signal (Singh et al., 2012) which can be recorded, monitored, or processed in real-time for biomedical applications. Such signals are continuous in nature, but sampled in a discrete set of observations with a temporal resolution which directly depends on the sampling rate of the recording device. The higher the sampling frequency, the higher the number of observations per time unit, and the better the approximation to the local shape of the data.

In the field of neurophysiology, electroencephalography (EEG) represents one of the few techniques providing a direct measure of bio-electrical brain activity, as oscillations in excitability of populations of cortical pyramidal cells (Wang, 2010) contribute to variations in the electrical potentials over the scalp. Oscillations are characterized by dominant intrinsic rhythms conventionally grouped into frequency bands, which are by now validated as markers of several neurocognitive

phenomena (Buzsáki, 2006). However, despite the temporal resolution achievable with its high sampling rate, EEG is a technique that suffers from low signal-to-noise ratio. This is mainly due to the fact that the layers of tissue dividing the electrodes from the cortex act as a natural filter attenuating genuine brain activity and mixing the sources: due to volume conduction, the activity originating from each single dipole is picked up by electrodes at all scalp locations fading as a function of distance from the origin (Nunez and Srinivasan, 2006). Furthermore, the dominant brain-related spectral features often overlap with artifactual activity in higher frequency bands (Castellanos and Makarov, 2006; Muthukumaraswamy, 2013), and particularly at lower frequencies most of the variance in the signal is explained by physiological sources outside the brain. For these reasons, analyzing EEG signals can ultimately be viewed as solving a source-separation problem with the goal of estimating brain potentials of interest.

Blind source separation (BSS) techniques such as independent component analysis (ICA) are commonly used to address artifact detection and correction of EEG signals. The term ICA encompasses a broad scope of algorithms and theoretical rudiments aligned to the assumption of independence of the underlying sources. ICA might be generally defined as an unsupervised statistical tool used to isolate mutually independent components from a sample assumed to be generated by a mixture of unknown marginal distributions. From the statistical perspective, it could be regarded as an extension of principal component analysis (PCA) that goes beyond the variance patterns of the data introducing high order statistical measures such as kurtosis or negentropy. Since the ICA problem was framed in Hervé and Jutten (1986), the technique has taken the form of sophisticated algorithms with varying approaches. In fact, the study of the artifactual activity from observed multivariate EEG signals can be performed by a wide collection of BSS algorithms. Among the most popular, we mention fastICA (Hyvärinen and Oja, 1997), Infomax (Bell and Sejnowski, 1995) or the joint approximate diagonalisation of eigenmatrices (JADE, Cardoso and Souloumiac, 1993). In this paper, however, we will tackle the separation of source artefacts using the fourth-order blind identification (FOBI, Cardoso, 1989), which is a classical solution based on the decomposition of the kurtosis matrix or the weighted covariance. Our choice is motivated by recent extensions of this method to the functional data paradigm. Indeed, the FOBI estimator has interesting properties (see for a review Nordhausen and Virta, 2019) and is of easy computation, which makes it a suitable method to explore and generalize ICA framework in functional spaces. We will use this kind of data to prove the validity of the method at extracting physiological artifacts.

Functional data analysis (FDA) is a branch of modern statistics with active research in methodological developments for sampling units in form of functions instead of vectors of measurements as in multivariate analysis. In practice, however, curves are observed in a finite set of sampling points and thereby the first step in FDA is to convert these values into a functional structure that mimics the original (continuous) nature of the sample paths. As functional data is inherently infinite-dimensional, generalizations of multivariate objects such as inverses become an important issue which complicates the implementation of ICA in functional spaces. In this paper, we consider the projection of the sample curves on a finite-dimensional space generated by a suitable basis of functions in order to solve the ICA problem in functional terms.

The use of functional data in brain imaging analysis has gained notoriety in the last years despite the problems arisen in its application. These include a considerable computational cost due to the large volume of data and the highly multicollinearity of electrode signals in regional dense spatial sets. Moreover, the assumption of normality of the error term in the functional model (see 1) should not be taken pragmatically as it can be biased due to sources of noise originated by non-neuronal agents (Tian, 2010). On the other end, data acquired from EEG might elicit a wide variety of FDA methods, going from the estimation of smoothing sample curves to more advanced reduction and prediction techniques. An application of FDA to EEG data was proposed in Pokora et al. (2018) to study Auditory Evoked Potentials (AEPs) using cross distance measures on functional responses and its derivatives approximated by cubic smoothing B-splines. Scheffler et al. (2018) introduced

a novel hybrid principal component analysis (HPCA) for high-dimensional data consisting of a PCA in the frequency domain along regional dimensions (electrode group) combined with a functional PCA in the longitudinal and functional dimension assuming, in the decomposition, the notion of weak separability among marginal covariances. This procedure is beneficial in a sense that it avoids collapsing sparse data in any of the considered dimensions. Similarly, [Hasenstab et al. \(2017\)](#) proposed a multidimensional functional PCA that preserves the singularity of the Event Related Potentials (ERPs) over the longitudinal domain from its moving average. EEG data was also used in the context of functional linear regression to test a supervised version of functional PCA ([Nie et al., 2018](#)). As noted, most of the FDA methods used in EEG brain studies are focused on modelling data free of artifactual sources. However, the efficiency of FDA as a signal pre-processing tool in stages where data is contaminated by physiological artifacts remains, to the best of our knowledge, not yet been tested.

During the past decade, neurocognitive research started to move towards ecological, mobile and interactive experimental scenarios ([Gramann, 2014](#)). In this context, full-body movements such as gait, trunk sway and arm gestures are likely to exacerbate the artefacts most commonly encountered in neurocognitive research (e.g., blinks, ocular movements, temporo-mandibular muscular activity, sweat, etc.), and bring into the scenario high-amplitude mechanical artefacts due to cable movements. Given the need for overcoming these issues, we propose a framework which accounts for both the most stereotyped artifacts and the ones strictly related to body movement. In order to demonstrate its validity, we reproduced a typical experimental scenario where a human participant had to perform full-arm movements synchronised to a periodic auditory stimulus during an EEG recording. Arguably, what we provide here is a paradigmatic example wherein the researcher needs to clean the signal from motion-related artefacts, while preserving activity genuinely related to perceptual and motor brain processes.

Nevertheless, the main contribution of this work does not end with an ordinary estimation and removal of these artifacts; we propose a functional-valued denoising tool based on B-spline expansions that takes advantage of the FDA smoothing techniques to preserve high-frequency remnants of neural origin overlapping latent artifactual sources. An earlier work that might resemble to our method applies directly to the data the discrete wavelet transform (DWT) using different levels of decomposition to smooth the approximation coefficients in order to obtain ocular artifacts free of neural data ([Kelly et al., 2011](#)). Further approaches combine the wavelet decomposition and ICA to denoise the captured artifactual components ([Akhtar et al., 2012](#); [Mahajan and Morshed, 2015](#)). In spite of the obvious differences between both data kinds, our ICA model provides a component estimation based on a P-spline smoothed approach ([Eilers and Marx, 1996](#); see also [Xiao, 2019](#)), which has a lower computational cost and is mathematically simpler. Moreover, in the proposed method, smoothing is the primary property that prompts the FICA decomposition of the EEG signal rather than an auxiliary strategy used to correct the estimates. However, what differentiates our method from others is that the decomposition is naturally regulated by the principal component eigendirections and optimized by means of penalized estimators whereas in using wavelet decomposition this is decided on the basis of a frequency band features of the data or the components, as the case may be. The end user will finally appreciate how artifact extraction can be fine-tuned by regulating a single smoothing parameter, making it intuitive to improve the outcomes by means of a visual inspection of the independent component scores.

The paper is organized as follows. In Section 2 we start by defining the FICA framework from an infinite-dimensional space perspective to further develop the theoretical foundations of our model. Section 3 introduces the novel regularized FICA decomposition from the basis expansion representations of functional data. An innovative method for the selection of the model parameters based on the normalized kurtosis of the independent component vectors is also proposed. To prove the performance of our methods, in Section 4 we use real EEG data on a single and group-level ERP designs. We also provide guidelines and the procedure for artifact detection and removal to get clean EEG functional data. Finally, some concluding remarks and prospective research directions

are presented in Section 6.

## 2 Functional ICA of the finite Karhunen-Loève expansion

The extension of ICA to functional data has not yet received the attention nor the prolific developments of its predecessor, the functional principal component analysis (FPCA). A first attempt to implement independent techniques for functional data was proposed in [Peña et al. \(2014\)](#), where the kurtosis (FOBI) operator is defined as an estimator over an approximation to a separable infinite-dimensional Hilbert space. In this space setting, the independent component weight functions are expected to be rougher as it does not contain functions that are pointwise convergent. Their approach focuses on the classification properties of the kurtosis operator, whose decomposition is assumed to have a form similar to the Fisher discriminant function.

A version of functional ICA based on the FOBI method that can be regarded as an extension of its multivariate counterpart was first developed in [Li et al. \(2015\)](#). The distinctive aspect that characterizes the model is that the ICA procedure starts from the Karhunen-Loève (K-L) expansion ([Ash and Gardner, 1975](#), p. 37), which is a less rough version of the original sample space since it steems from its optimality in the least-squared error sense. We extend this model, which throughout the paper is referred as *functional ICA in terms of principal components* or KL-FICA, endowing the space with a different geometrical structure given by a Sobolev inner product to control the roughness of the latent functions. In a sense, both approaches can be considered a refinement of [Peña et al. \(2014\)](#). More recently, [Virta et al. \(2020\)](#) proposed a version of the KL-FICA model for multivariate functional data using FOBI and JADE estimators.

### Basic model setup

Let  $x_i = (x_{i1}, \dots, x_{im_i})^\top$  be a signal of  $i, (i = 1, \dots, n)$  components digitized at the sampling point  $t_{ik}, (k = 1, \dots, m_i)$ . Consider that the sample data is observed with error, so that it can be modeled as

$$x_{ik} = \chi_i(t_{ik}) + \varepsilon_{ik} \quad (1)$$

where  $\chi_i$  is the  $i$ -th functional trajectory of the signal and  $\varepsilon_{ik}$  mutually independent measurement errors with zero means. The functions  $\chi_1, \dots, \chi_n$  are assumed to be independent and identically distributed copies of a random functional variable  $X$  in  $L^2(T)$ , the separable Hilbert space of square integrable functions from  $T$  to  $\mathbb{R}$ , endowed with inner product  $\langle \cdot, \cdot \rangle$  and the induced norm  $\|\cdot\|$ . Throughout the text,  $X$  is assumed to have zero mean and finite fourth moments, i.e  $E \|X\|^4 < \infty$ , which implies that higher order operators are well defined.

The concept of independent components of a random vector cannot be immediately extended to the case of Hilbert-valued random elements (functional data) due to the fact that a probability density function is not generally defined in this context. Here, we use the definition of independence first introduced by [Gutch and Theis \(2012\)](#); [Li et al. \(2015\)](#) in the ICA framework for infinite-dimensional spaces, which basically states that a random functional variable has independent components if the coordinates obtained after projecting into a given orthonormal basis are independent variables. Then, the aim of FICA is to find an operator  $\Gamma$ , such that  $\langle \Gamma X, f_j \rangle, (j = 1, \dots, q)$  are mutually independent variables with  $\{f_j : j \in q\}$  being a truncated orthonormal basis in  $L^2(T)$ . As functional data is not inherently Gaussian, our IC model is based on the assumption that if  $X$  is approximately represented by a truncated orthonormal basis, then it admits the FICA decomposition. Otherwise, by considering  $X$  prompted by a Gaussian process, a FPCA will suffice to obtain the independent components ([Ash and Gardner, 1975](#), p. 40). This IC model begs inevitably to the question of the basis choice. In our FICA approach, the sample curves are reconstructed using the K-L expansion, meaning that the chosen basis is provided by the decomposition of the covariance operator.

For an arbitrary function  $h \in L^2(T)$  and  $s \in T$ , we define the sample covariance operator as

$$\mathcal{C}(h)(s) = n^{-1} \sum_{i=1}^n \langle \chi_i, h \rangle \chi_i(s) = \langle C(s, \cdot), h \rangle,$$

which induced by the covariance kernel of  $\chi$ ,  $C(s, t) = n^{-1} \sum_{i=1}^N \chi_i(s) \chi_i(t)$ ,  $t, s \in T$ , transforms  $h$  into another function of  $L^2(T)$ . Then, Mercer's theorem provides the eigendecomposition

$$C(s, t) = \sum_{j=1}^{\infty} \eta_j f_j(s) f_j(t),$$

denoting by  $\{\eta_j, f_j\}_j$  the positive sequence of eigenvalues in descending order and their associated orthonormal eigenfunctions. As a remainder, observe that when the kernel is hermitian (symmetric) and positive-definite, the uniformly converging series expansions are obtained for both kernel and its associated operator. It follows that, for every  $t \in T$ , we can approximately represent  $\chi_i(t)$  by a truncated series of the K-L expansion

$$\chi_i^q(t) = \sum_{j=1}^q z_{ij} f_j(t),$$

where  $z_{ij} = \langle \chi_i, f_j \rangle$  are zero mean random variables with  $\text{var}(z_j) = \eta_j$  and  $\text{cov}(z_j, z_{j'}) = 0$  for  $j \neq j'$ . These variables are referred to as the principal components scores. Moreover, if the  $q$  term of the K-L is optimally selected, the mean squared error is minimized (Ghanem and Spanos, 1991, p. 21), providing the best linear approximation to  $\chi_i(t)$ .

Our main assumption facts that the target functions can be found in the space spanned by the first  $q$  eigenfunctions of  $\mathcal{C}$ , as it is endowed with a second-order structure represented by the major modes of variation of  $\chi_i(t)$ . Thus, in such eigensubspace it is expected to gain some accuracy in the forthcoming results due to the attenuation of the higher oscillation modes corresponding to the small eigenvalues of  $\mathcal{C}$ . In the following, we denote  $\mathcal{H}^q = \text{span}\{f_1, \dots, f_q\}$  the subspace spanned by the  $q$  first eigenfunctions of  $\mathcal{C}$ , which form the chosen basis for our IC model. Without loss of generality,  $\mathcal{H}^q$  will be assumed to preserve the inner product in  $L^2(T)$ .

Most of the multivariate ICA methods require the standardization of the observed data with the inverse square root of the covariance matrix in order to remove any linear dependencies and normalize the variance along its dimensions. In infinite-dimensional spaces, however, covariance operators are not invertible giving rise to an ill-posed problem. As long as our signal is represented in  $\mathcal{H}^q$ , no regularization is needed and consequently, the inverse of the covariance operator can be well defined. Then, the first step towards the estimation of the independent components consists of a transformation of the K-L coefficients (PCs) with respect to the usual Euclidean geometry. Since standardization is a particular case whitening (or spherling), we can generalize the procedure in the form of a whitening operator  $\Psi$  that transforms a function in  $\mathcal{H}^q$  into a standarized function on the same space. This implies that  $\Psi(\chi^q) = \tilde{\chi}^q$  is a standarized functional variable whose covariance operator  $\mathcal{C}_{\tilde{\chi}^q}$  naturally satisfies to be the identity inside the space.

By analogy to the FPCA, it follows the decomposition of the FOBI operator (kurtosis), which is defined as

$$\mathcal{K}(h)(s) = n^{-1} \sum_{i=1}^n \langle \tilde{\chi}_i^q, \tilde{\chi}_i^q \rangle \langle \tilde{\chi}_i^q, h \rangle \tilde{\chi}_i^q(s) = \langle K(s, \cdot), h \rangle, \quad (2)$$

where  $K(s, t) = n^{-1} \sum_{i=1}^n \|\tilde{\chi}_i^q\|^2 \tilde{\chi}_i^q(s) \tilde{\chi}_i^q(t)$ ;  $s, t \in T$  denotes the FOBI kernel function of  $\tilde{\chi}^q$  and  $h$ , the function in  $\mathcal{H}^q$  to be transformed. As in Li et al. (2015), we assume the FOBI operator to be positive-definite, hermitian and equivariant such that there exists the eigendecomposition

$$K(s, t) = \sum_{l=1}^q \alpha_l g_l(s) g_l(t), \quad l = 1, \dots, q,$$

where  $\{\alpha_l, g_l\}_l$  is a positive sequence of distinct eigenvalues and related eigenfunctions.

With this, we are now ready to define the independent components of  $\chi_i^q$  as generalized linear combinations with maximum kurtosis given by  $\zeta_{il,\tilde{x}} = \langle \tilde{\chi}_i^q, g_l \rangle$ . Challenging questions arise on how the Karhunen-Loève theorem might be applied in this context. Intuitively, we note that this procedure leads to the expansion  $\tilde{\chi}_i^q(t) = \sum_{l=1}^q \zeta_{il,\tilde{x}} g_l(t)$  which can also be approximated in terms of  $r$  eigenfunctions  $g_l$  of interest, e.g. those associated with the independent components with the most extreme kurtosis values. Under mild conditions, this problem was solved in [Li et al. \(2015\)](#); [Virta et al. \(2020\)](#) by choosing  $r = q$ . However, there are other possibilities, such as consider  $r < q$  or  $g_l$  as a basis of projection for either  $\chi$ ,  $\chi^q$  or  $\tilde{\chi}^q$ , in view of the fact that it preserves the four-order structure of the standardized data. In our EEG study, we propose to project the original functions on the basis  $\{g_1, \dots, g_q\}$  to discern artifactual patterns. We then subtract the space generated by a basis of selected artifactual eigenfunctions from the original curves to obtain a new sample that can be regarded as an estimate of the genuine brain activity.

### 3 P-spline smoothed KL-FICA: basis expansion estimation

[Silverman \(1996\)](#) introduced a method that combines the use of the  $d$ -order differential operator to control the roughness of the weight functions in order to estimate smooth (or regularized) functional principal components. By this heuristic, it incorporates a fixed roughness penalty into the orthonormality constraint between principal components, unlike other approaches that penalize the variance ([Rice and Silverman, 1991](#)) or the covariance operator ([Yao et al., 2005](#)). In [Aguilera and Aguilera-Morillo \(2013b\)](#) two alternative versions of smoothed FPCA are discussed, taking advantage of a discrete penalization in terms of adjacent B-spline coefficients (P-spline penalty). In a sense, the smoothed functional ICA considered here is based on the second FPCA version in [Aguilera and Aguilera-Morillo \(2013b\)](#) which incorporates the P-spline penalty in the orthonormality constraint.

In order to estimate the P-spline smoothed PCs, we assume next that the sample paths belong to a finite analogue of the Hilbert space  $L^2(T)$  spanned by a basis  $\{\phi_1(t), \dots, \phi_p(t)\}$ . Each function of the sample can be expanded as  $\chi_i(t) = \sum_{j=1}^p a_{ij} \phi_j(t)$ , where  $a_{ij}$  are random coefficients. In matrix form,  $\chi = \mathbf{A}\phi$ , where  $\mathbf{A}$  is the coefficient matrix  $\mathbf{A} = (a_{ij}) \in \mathbb{R}^{n \times p}$  associated to the basis  $\phi = (\phi_1, \dots, \phi_p)^\top$ , with  $\chi = (\chi_1, \dots, \chi_n)^\top$ . For the rest of this section, we consider that the sample curves are expanded in terms of B-spline basis functions.

Under the model (1), the basis coefficients of sample curves can be found by least squares approximation minimizing the Mean Squared Error (MSE) for each  $i$ , i. e.,

$$(\hat{a}_{i1}, \dots, \hat{a}_{ip})^\top = \operatorname{argmin} \sum_{k=1}^{m_i} \left\{ \chi_{ik} - \sum_{j=1}^p a_{ij} \phi_j(t_{ik}) \right\}^2,$$

and thus, the estimate of  $\mathbf{a}_i = (a_{i1}, \dots, a_{ip})^\top$  that minimizes the MSE is  $\hat{\mathbf{a}}_i = (\Phi_i^\top \Phi_i)^{-1} \Phi_i^\top \chi_i$ , where  $\Phi_i = \{\phi_j(t_{ik})\} \in \mathbb{R}^{m_i \times p}$ . For general guidance on both basis selection and its order, we refer the reader to Chapters 3 and 4 in [Ramsay and Silverman \(2005\)](#). Although in this paper it is assumed a non-penalised B-spline basis to approximate the functional representations of the data, [Aguilera and Aguilera-Morillo \(2013a\)](#) give a detailed account of how to solve it using different roughness penalty approaches (continuous and discrete) for estimating curves in terms of B-spline basis.

The truncated K-L expansion is generated by the first  $q$ -eigenfunctions ( $q \leq p$ ) of the covariance operator, which are given in terms of the B-spline basis as

$$f(t) = \sum_{k=1}^p b_k \phi_k(t) = \phi(t)^\top \mathbf{b},$$

with  $\mathbf{b} = (b_1, \dots, b_p)^\top$  being its vector of basis coefficients. The discrete P-spline roughness penalty function is defined by  $\operatorname{PEN}_d(f) = \mathbf{b}^\top \mathbf{P}_d \mathbf{b}$ , where  $\mathbf{P}_d$  is a matrix of penalties given by

$$\mathbf{P}_d = (\Delta_d)^\top \Delta_d,$$

with  $\Delta_d$  being the matrix representation of the  $d$ -order difference operator. Throughout the paper it is usually assumed a penalty order of  $d = 2$  which is equivalent to

$$\mathbf{b}^\top \mathbf{P}_2 \mathbf{b} = (b_1 - 2b_2 + b_3)^2 + \cdots + (b_{p-2} - 2b_{p-1} + b_p)^2,$$

so that the difference matrix  $\Delta^2$  has the form

$$\Delta^2 = \begin{bmatrix} 1 & -2 & 1 & 0 & \cdots \\ 0 & 1 & -2 & 1 & \cdots \\ 0 & 0 & 1 & -2 & \cdots \\ \vdots & \vdots & \vdots & \vdots & \ddots \end{bmatrix}.$$

According to [Aguilera and Aguilera-Morillo \(2013b\)](#); [Silverman \(1996\)](#), the weight functions  $f$  are determined by maximizing  $\text{var}\langle f, x \rangle$  subject to orthonormality with respect to the Sobolev type inner product given by  $\langle g, h \rangle_\lambda = \langle h, g \rangle + \lambda \mathbf{h}^\top \mathbf{P}_d \mathbf{g}$ , with  $\mathbf{h}$  and  $\mathbf{g}$  being the vectors of basis coefficients of the functions  $h(t)$  and  $g(t)$ , respectively. This is equivalent to maximize the penalized sample variance defined by

$$\frac{\text{var}\langle f, x \rangle}{\langle f, f \rangle + \lambda \times \text{PEN}_d(f)} = \frac{\mathbf{b}^\top \mathbf{\Theta} \mathbf{\Sigma}_A \mathbf{\Theta} \mathbf{b}}{\mathbf{b}^\top (\mathbf{\Theta} + \lambda \mathbf{P}_d) \mathbf{b}}, \quad (3)$$

where  $\mathbf{\Theta} = (\langle \phi_j, \phi_{j'} \rangle)$ ,  $(j, j' = 1, \dots, p)$ ,  $\mathbf{\Sigma}_A = \frac{1}{n} \mathbf{A}^\top \mathbf{A}$  and  $\lambda \geq 0$  is a penalty parameter that controls the trade-off between maximizing the sample variance and the strength of the penalty.

Because B-spline basis are non-orthogonal with respect to the usual  $L^2$  geometry (inner product), we can apply Choleski factorization of the form  $\mathbf{L} \mathbf{L}^\top = \mathbf{\Theta} + \lambda \mathbf{P}_d$  in order to find a non-singular matrix that allows us to operate in terms of the B-spline geometrical structure induced into  $\mathbb{R}^q$ . Then, the solution leads to an eigenproblem of a Hermitian matrix

$$\mathbf{L}^{-1} \mathbf{\Theta} \mathbf{\Sigma}_A \mathbf{\Theta} \mathbf{L}^{-1\top} \mathbf{v}_j = \eta_j \mathbf{v}_j, \quad (4)$$

to compute the coefficients of the weight functions as  $\mathbf{b}_j = \mathbf{L}^{-1\top} \mathbf{v}_j$ , and renormalized so that  $\mathbf{b}_j^\top \mathbf{\Theta} \mathbf{b}_j = 1$ . The  $j$ -th smoothed principal component is then obtained as  $\mathbf{z}_j = \mathbf{A} \mathbf{\Theta} \mathbf{b}_j$ . Under this framework, the multivariate PCA of  $\mathbf{A} \mathbf{\Theta} \mathbf{L}^{-1\top}$  in  $\mathbb{R}^q$  and the P-spline smoothed FPCA of  $x(t)$  in  $L^2(T)$  are equivalent (see section 4 in [Aguilera and Aguilera-Morillo, 2013a](#)).

Having estimated the weight functions coefficients and principal components scores, assume next that the smooth K-L expansion is truncated at the  $q$ -term, e.g. we may choose  $q = p$ . Then, the vector of sample curves is given by  $x^q(t) = \mathbf{Z} f(t)$ , where  $\mathbf{Z} = (z_{ij}) \in \mathbb{R}^{n \times q}$  is the matrix of principal components coefficients (scores) with respect to the basis of smooth PC weight functions  $f(t) = (f_1(t), \dots, f_q(t))^\top$ .

Following the ICA pre-processing steps, we first standardize the approximated K-L curves defining the whitening operator as  $\tilde{x}^q(t) = \Psi\{x^q(t)\} = \tilde{\mathbf{Z}} f(t)$ , with  $\tilde{\mathbf{Z}} = \mathbf{Z} \mathbf{\Sigma}_Z^{-1/2}$  being the matrix of standardized PCs and  $\mathbf{\Sigma}_Z^{-1/2} = \sqrt{n}(\mathbf{Z}^\top \mathbf{Z})^{-1/2}$ , the inverse square root of the covariance matrix of  $\mathbf{Z}$ . As the described whitening transformation is essentially an orthogonalization of the probabilistic part of  $x^q$ , now the matrix  $\tilde{\mathbf{Z}} \in \mathbb{R}^{n \times q}$  satisfy  $\mathbf{\Sigma}_{\tilde{\mathbf{Z}}} = \mathbf{I}_q$ .

Second, the diagonalization of the FOBI operator (expression 2) of the standardized K-L curves  $\tilde{x}^q(t)$  leads to the diagonalization of the FOBI matrix of the standardized PCs  $\tilde{\mathbf{Z}}$  as

$$\mathbf{\Sigma}_{4, \tilde{\mathbf{Z}}} \mathbf{u}_l = \alpha_l \mathbf{u}_l, \quad l = 1, \dots, q, \quad (5)$$

where  $\mathbf{\Sigma}_{4, \tilde{\mathbf{Z}}} = \frac{1}{n} \sum_{i=1}^n \|\tilde{\mathbf{z}}_i\|^2 \tilde{\mathbf{z}}_i \tilde{\mathbf{z}}_i^\top = \frac{1}{n} \tilde{\mathbf{Z}}^\top \mathbf{D}_{\tilde{\mathbf{Z}}} \tilde{\mathbf{Z}} \in \mathbb{R}^{q \times q}$ , with  $\mathbf{D}_{\tilde{\mathbf{Z}}} = \text{diag}(\tilde{\mathbf{Z}} \tilde{\mathbf{Z}}^\top)$ , and  $\tilde{\mathbf{z}}_i$  being the column vector  $q \times 1$  with the  $i$ -th row of the matrix  $\tilde{\mathbf{Z}}$ . This means that the P-spline smoothed KL-FICA of  $x(t)$  is obtained from the multivariate ICA of  $\mathbf{Z}$  in  $\mathbb{R}^q$ .

Expression (5) is not restricting to assume that  $\mathbf{\Sigma}_{4, \tilde{\mathbf{Z}}}$  is uniquely determined, in fact, several different definitions has been proposed since the classical formulation in [Cardoso \(1989\)](#). It is also worthy to note the kurtosis matrix in [Kollo \(2008\)](#),

$$\mathbf{\Sigma}_{4, \tilde{\mathbf{Z}}} = n^{-1} \sum_{i=1}^n \tilde{\mathbf{z}}_i \mathbf{1}_q^\top \mathbf{1}_q \tilde{\mathbf{z}}_i^\top \tilde{\mathbf{z}}_i \tilde{\mathbf{z}}_i^\top + (q+2) \mathbf{I}_q,$$

which includes all mixed fourth moments by incorporating all-one vectors, or the matrix proposed in Loperfido (2017) based on the dominant eigenpair of the fourth standardized moment. This FOBI extensions will be discussed in a future paper.

This way, the KL-FICA decomposition of  $x$  is already obtained. The IC weight functions are now expressed as  $g_i(t) = \sum_{j=1}^q u_{ij} f_j(t)$ , ( $i = 1, \dots, q$ ), where the coefficients vectors  $u_i$  are the eigenvectors of the predefined kurtosis matrix. Then, the independent components are obtained as  $\zeta_{i,\tilde{x}} = \tilde{\mathbf{Z}} u_i$ . Finally, the operator  $\Gamma$  defining the FICA model is given by  $\Gamma(x_i^q) = \mathbf{f}^\top \mathbf{U}^\top \Sigma_{\mathbf{Z}}^{-1/2} \mathbf{z}_i$ , with  $\mathbf{z}_i$  being the column vector  $q \times 1$  with the  $i$ -th row of the matrix  $\mathbf{Z}$ .

### Choosing $q$ according to the kurtosis excess of the coordinate vectors

The problem concerning the estimation of the independent component curves lies in the fact of finding an optimal truncation point of the K-L expansion and in an appropriate selection of the penalty parameter. When  $q$  approaches to  $p$ , more of the higher oscillation modes of the standardized sample are induced in the estimation. Otherwise, we are denoising the weight functions from the fourth-order structure of the data. From this perspective, it is desirable to increase the value of  $q$  such that the latent functions from the whitened space can be captured (Virta et al., 2020). Observe that this kind of regularization is not exactly the same as the one providing the P-spline penalization of the roughness of the weight functions. Attenuating the higher frequency components of the FPCA model does not necessarily affect an entire frequency bandwidth of the data. Thus, if the original curves are observed with independent error, it may overlap the estimation of the weight functions. In this context, smoothing would be appropriate. Once the value of  $q$  is chosen, we should examine those components with kurtosis excess, contrary to the FPCA where the components associated to large eigenvalues are considered.

We next propose a new method to approach  $q$  defining a fourth-moment measure which expresses the degree of kurtosis excess on a given independent component coordinate space. Assume this space to be  $\zeta_{i,\tilde{x}} = \langle \tilde{x}_i^q, g_i \rangle$ , i.e. the projection of the standardized original sample curves on the FOBI basis estimated from the FICA decomposition of  $x$ . In this independent setting, seems more reasonable to evaluate the non-gaussianity of the component vectors as they provide the most direct eigenfunction contribution to the original sample. Then, to calculate the degree of kurtosis excess in ICs, we define a fourth-moment measure given by

$$KE_q = \left\| \left\{ \text{kurt}(\zeta_{i,\tilde{x}}) \right\}_{i=1}^q \right\|,$$

where  $\zeta_{i,\tilde{x}}$  is the  $i$ -th IC and  $\text{kurt}(\zeta_{i,\tilde{x}}) = n^{-1} \sum_{i=1}^n \left\{ \left( \zeta_{i,\tilde{x}} - \bar{\zeta}_{i,\tilde{x}} \right) / \sigma(\zeta_{i,\tilde{x}}) \right\}^4 - 3$ , which gives the normalized excess of kurtosis for each IC. Then the value of  $q$  is selected according to

$$\underset{1 < q \leq p}{\text{argmax}} (KE_q), \quad (6)$$

for  $q$ -FICA decompositions of  $x$ . In our EEG example, (6) is iterated until the velocity of the eigenvalues  $\Delta \{ \eta_1, \eta_2, \dots, \eta_p \}$  associated to the FPCA of  $x$  ceases locally to increase in the neighbourhood of the dominant eigenvalue. Velocity fluctuations can occur in the exponential decay of  $\eta_j$ , meaning that, asymptotic stability is not necessarily being reached using this criterion. We do find, however, that this is a way of exploring independence in the high variability structure of our data, but it also goes to ensure that the FICA decomposition induces enough independent-part of the model to separate the latent functions without losing accuracy in its estimation. In analysing EEG signals, this entails a major effectiveness in reducing the artifactual content to a few eigenfunctions, particularly for low-frequency physiological activity such as blinks and motor artifacts. The presence of other high-frequency muscular artifacts, however, poses the researcher in a more challenging situation. The choice of an appropriate truncation point should be seen as a measure to improve the accuracy of the estimation of those artifacts as to preserve modes of variability related brain activity rhythms. We believe that, instead of adjusting  $q$  to larger values of cumulated variance, an iterative FICA process to scale artifact removal may be considered to solve the problem.

## Penalty parameter selection

Leave-one-out cross validation (CV) is generally used to select the penalty parameter in order to achieve a desirable degree of smoothness of the weight functions. In a more explicit and condensed form, the CV procedure in our model lies in finding a value of  $\lambda$  that minimizes

$$CV_q(\lambda) = \frac{1}{n} \sum_{i=1}^n \left\| \chi_i - \chi_i^{q(-i)} \right\|^2, \quad (7)$$

where  $\chi_i^{q(-i)} = \sum_{l=1}^q z_{il}^{(-i)} f_l^{(-i)}$  is the K-L representation of the  $i$ -th curve  $\chi_i$  in terms of the  $q$  first principal components by leaving out it in the estimation process. This method can be combined with (6) so that once  $\lambda$  is chosen for each fixed  $q$ , then the optimum  $q$  is the one that maximizes  $KE_q$ .

Here, an important remark has to be made about the regularization of the weight functions. [Castellanos and Makarov \(2006\)](#) and references therein (see section 2.6) discuss about the reliability of the estimated artifactual sources as they are assumed to contain traces of independent leaked cerebral activity. Such assumption complicates things when oscillations related to brain rhythms are yet observable on the estimated IC weight functions. Moreover, we found that cross validation was not sensitive for a reasonably large basis dimension, forcing us to reformulate the strategy. To address this issue, the penalty parameter might be subjectively chosen to the suitable degree of smoothness, however, this can lead in a distortion and poor extraction of the artifactual sources. For the results presented in this paper, we propose a novel adaptation of cross validation which consists in replacing (7) by:

$$BCV_q(\lambda) = \frac{1}{n} \sum_{i=1}^n \left\| \chi_i^{q;\lambda(-i)} - \chi_i^{q;\lambda+\ell(-i)} \right\|^2, \quad (8)$$

where  $\chi_i^{q;\lambda(-i)}$  is a smoothed K-L representation for some  $\lambda$  and  $\ell > 0$  a value that increases the smoothing in the second term of the norm, assume  $\ell = 0.1$ . For a fixed  $q$ , (8) is iterated for a set of  $\lambda$ 's to find which minimizes  $BCV_q(\lambda)$  and provide the choice of the penalty parameter. Similarly as in (7), it can be combined with (6) to select the most suitable  $q$  via maximizing  $KE$ .

We call this method *baseline cross validation*, as it operates across different K-L reconstructions of  $\chi_i$  for a given baseline penalty parameter and a fixed  $q$ . This approach is more versatile and particularly useful when the original curves are extremely rough and have been approximated with a larger basis dimension. In addition, for a given  $q$  it lets score more than one  $\lambda$  as a result of the various relative minima it produces. The intuition behind baseline cross validation is that there are several levels of smoothing to endow the estimator with the ability for predictive modelling. Thus, the selection of the value that minimizes it is a merely practical matter in this work. The implementation of the method for a larger basis order using shrinkage estimators is given in Section 4. Let us remind that no categorical rules are provided here for the selection of  $\lambda$  as the physiological significance of smoothing is not tested in this paper; this is a matter for a future research.

Further complication arises in evaluating the relationship between the kurtosis excess and the selected penalty parameter, from which  $KE$  for some  $\lambda$  is expected to be optimized with respect to  $\lambda = 0$ . In general, we advocate to dismiss smoothing if  $KE$  diminishes, as it would represent that regularization is naturally optimized in the sense of the principal eigendirections, and therefore the induced roughness may be attributable to the independent part of the model. In other words, the latent functions strongly depend on the induced noise to shape a more accurate independent space structure. However, this rule will be relaxed in order to estimate low-frequency artifactual curves free of persistent brain activity, even though it does come with the price of losing other interesting artifacts.

## 4 Application to EEG data

We now discuss the efficacy of our method in estimating artifactual functions on real EEG data. A first use case is proposed in the context of event-related potentials (ERPs) analysis, where the

researcher preferably deals with a high number of short time series aligned to some event. We begin this section by describing the data and the method to reconstruct the functional form of the sample paths. Then, we analyze distinct short recordings containing common artifacts of induced movements and propose a procedure for artifact detection, correction and subtraction. The ordinary and penalized KL-FICA are compared. Finally, we propose an automated method for a group of functional ERPs.

### Materials and experimental design

EEG data were recorded across different conditions from a single healthy subject (male, 35 years old) with a 64-channels *eego™mylab* system, in the Art Science and Interaction Lab (ASIL) of Ghent University (Belgium). In a first session, the subject was sitting on a comfortable chair in front of a table and instructed to perform the following classes of self-paced movements in separate single-trials of 3 seconds: nodding, hand-tapping with a wide arm movement starting from the shoulder, eye-blinking and chewing. In a second session, the subject was instructed to tap his hand on the table synchronizing with a steady auditory stimulus in one condition, and to listen to the same stimulus in a condition without any movement involved. We recorded 100 trials per condition, divided in randomized blocks of 25 trials. The stimulus period was 750ms. Movements were intentionally exaggerated, to maximize eventual movement-related artifacts.

Our purpose was two-fold. With the first recording in absence of sensory stimulation, we aimed at isolating the stereotyped artifacts, and show how we can estimate and selectively remove them from heavily contaminated signal. In the second recording, we reproduced a minimal form of experimental design, contrasting a condition of listening while moving with a baseline condition of listening while sitting still. Disposing of a baseline, we could directly compare the outcome of our cleaning procedure with an uncontaminated experimental situation. Results will be shown on a selection of individual contaminated segments and on the grand-average ERPs for each condition. Any cognitive interpretation of the difference across conditions is beyond the scope of the present work.

### Methods

#### Pre-processing and general parameter tuning.

All recordings were performed with a sampling rate of 1 kHz, so for a trial length of 3 seconds we have 3000 sampling points. The signal was high-pass and low-pass filtered using Butterworth filters (cut-off at 0.5 and 30 Hz, order 4 and 6, respectively). An additional notch filter was applied for suppressing the 50 Hz power-line noise. For all the trials of the second recording, the filtered time series were baseline-corrected by subtracting the average of the -200 ms to 0 ms pre-stimulus from each time point.

Let  $x_i(t_{ik})$  denote the EEG potentials for the signal component  $i, (i = 1, \dots, 64)$  at time point  $t_{ik}, (k = 1, \dots, 3000)$  for each one single trial and  $2 \times 100$  trials whose FICA decompositions are conducted independently. In reconstructing the functional form of the sample paths, we sought a less smooth fitting, so we could mimic the brain potential fluctuations. Accordingly, a basis of cubic B-spline functions of dimension  $p = 230$  was fitted to all signal components minimizing the mean squared error of the estimation for the B-spline coefficients to a negligible value.

Since we require a basis dimension greater than the number of signal components (sample size), a shrinkage covariance estimator (Schäfer and Strimmer, 2005) is considered to compute  $\Sigma_A$  in the PCA algorithm. This method guarantees positive definiteness and consequently an estimation of the higher and important eigenvalues not biased upwards. The same strategy is used for baseline cross-validation. Recall the quadratic distances in (8). For the  $N$ -th trial, this distances in

terms of basis functions can be expressed as

$$\begin{aligned} \left\| \chi_i^{q;\lambda(-i)} - \chi_i^{q;\lambda+\ell(-i)} \right\|^2 &= \int_T \left[ \chi_i^{q;\lambda(-i)}(t) - \chi_i^{q;\lambda+\ell(-i)}(t) \right]^2 dt = \\ &= \int_T \left[ \sum_{l=1}^q z_{il}^{\lambda(-i)} \sum_{j=1}^p b_{lj}^{\lambda(-i)} \phi_j(t) - \sum_{l=1}^q z_{il}^{\lambda+\ell(-i)} \sum_{j=1}^p b_{lj}^{\lambda+\ell(-i)} \phi_j(t) \right]^2 dt = \int_T \left[ \sum_{j=1}^p c_{ij} \phi_j(t) \right]^2 dt = \mathbf{e}_i^\top \Theta \mathbf{e}_i, \end{aligned}$$

where  $\mathbf{e}_i = (e_{i1}, \dots, e_{ip})^\top$ . Next, the matrix  $\mathcal{E} = (\mathbf{e}_{ij}) \in \mathbb{R}^{n \times q}$  is reconstructed via shrinkage. That is, first we compute  $\text{cov}_S(C)$  where  $\text{cov}_S$  is the shrinkage covariance estimator, then we apply Cholesky decomposition of the form  $\mathbf{L} \mathbf{L}^\top = \text{cov}_S(\mathcal{E})$ . Finally, the basis coefficients of the reconstructed residual functions are given by  $\mathcal{E} \hat{\mathbf{e}}_i = \mathcal{E} \mathbf{L}^{-1} \mathbf{e}_i$ , and consequently now

$$\text{BCV}(\lambda)_q = \frac{1}{n} \sum_{i=1}^n \left\| \chi_i^{q;\lambda(-i)} - \chi_i^{q;\lambda+\ell(-i)} \right\|^2 = \hat{\mathbf{e}}_i^\top \Theta \hat{\mathbf{e}}_i.$$

The baseline cross-validation method combined with shrinkage estimators has resulted to be sensitive at larger basis dimension, but also provides insights within different levels of roughness of the sample curves at each  $q$ . For the present application, we will take the value that minimizes  $\text{BCV}(\lambda)_q$  for different values of  $q$  and use KE in its optimization.

#### Artifact detection and removal.

The process of identifying artifactual functions has not only been conducted by their suggested shape, also checked by using topographic maps that roughly represent patterns of eigenactivity related to the distribution of bio-electric energy along the scalp. These maps have been elaborated from the coordinates of the projection of  $\chi_i$  onto the basis of independent weight functions,

$$\zeta_{il,\chi} = \langle \chi_i, g_l \rangle, \quad l = 1, \dots, q, \quad (9)$$

whose resulting score vectors  $\zeta_{l,\chi} = (\zeta_{1l}, \dots, \zeta_{nl})^\top$  associated to each eigenfunction are depicted in the spatial electrode domain. Thus, the points in these maps represent energy markers color-coded for their positive or negative eigenfunction contribution to the each signal component  $\chi_i$ . Once the artifactual eigenfunctions have been identified, they can be manually selected together with their corresponding projection coefficients to reconstruct an expansion so that it can be subtracted from the original functional observations in order to remove the undesired artifactual curves. The projection coefficients where the selection is made are obtained from (9). In order to simplify the burden of a manual selection, assume

$$\chi_i^q(t) = \sum_{l=1}^q \zeta_{il,\chi} g_l(t),$$

to be an expansion of components corresponding to their related artifactual eigenfunctions. Then, the artifact subtraction in terms of basis expansions is given by

$$\chi_i(t) - \chi_i^q(t) = \sum_{j=1}^p a_{ij} \phi_j(t) - \sum_{l=1}^q \zeta_{il,\chi} \sum_{j=1}^p (\mathbf{u}_l^\top \mathbf{b}_j) \phi_j(t) = \sum_{j=1}^p d_{ij} \phi_j(t), \quad (10)$$

where  $d_{ij}$  are the residual (or cleaned) coefficients, with  $\mathbf{u}_l$  being the vector of coefficients of the independent weight function  $g_l$  in terms of the principal eigenfunctions, and  $\mathbf{b}_j$  being the vector of coefficients of the principal eigenfunctions in the basis  $\phi_j$ . This is equal to assume that all set of IC weight functions obtained from our model corresponds to an structure of underlying artifactual patterns of the EEG signal.

---

**Algorithm** KL-FICA estimation procedure for artifact reduction

---

1. Find a suitable B-spline representation of the sampled signal components. Estimate the matrix of coefficients  $A$  by least squares approximation.
2. Calculate the P-spline FPCA of  $\chi$ , or equivalently, the vector valued PCA of  $A\Theta L^{-1\top}$  to obtain the matrix of smooth principal components  $Z$  and the coefficients of the principal weight functions  $b_j$ .
  - (a) If  $p > n$ , consider shrinkage estimators to compute  $\Sigma_A$ .
  - (b) Obtain a  $\lambda$  for each  $q$  using BCV.
3. Perform the vector-valued ICA on the matrix  $Z$  for each  $q$ .
  - (a) Whiten the matrix of principal components:  $\tilde{Z} = Z\Sigma_Z^{-1/2}$ .
  - (b) Fix a fourth-order matrix  $\Sigma_{4,\tilde{Z}}$  and diagonalize it. Obtain the distinct eigenvalues  $\alpha_i$  and associated eigenvectors  $u_i$ .
  - (c) Calculate the components of interest by projecting the original observations on the basis of IC weight functions,  $\zeta_{i,\chi} = \langle \chi_i, g_i \rangle$  or simply  $\zeta_{i,\chi} = Z u_i$ .
4. Choose an optimal  $q$  using KE. Select manually the artifactual components (we consider all ICs) and expand the artifactual space.
5. Subtract the artifactual coefficients using (10) to obtain the coordinates of the cleaned signal components. Repeat the procedure for each trial.

---

## 5 Data analysis results

### Stereotyped artifacts

We first present full results of the unpenalized and penalized KL-FICA decomposition on the single-trials corresponding to motor related artifacts in absence of sensory stimulation. Baseline cross-validation was performed on a given grid of  $\lambda$ 's, selecting the value which minimizes  $BCV_q(\lambda)$  for  $(q = 1, \dots, j_0)$  where  $j_0$  is defined as  $\Delta\eta_{j_0} = \{j_0 : \max_1(\Delta\eta_j)\}$ , i.e. the index entry corresponding to the first relative maxima of FPCA eigenvalues in first differences. Among all the results obtained, we selected the  $q$  that for its corresponding estimated  $\lambda$  maximizes KE.

Our preliminary results comparing both decompositions show that the smoothed KL-FICA provides more stylised functions revealing the latent form of the artifact. More importantly, however, is that all topographic maps of the chosen components reflect well-known spatial firings of the expected artifactual activity. A selection of eigenfunctions from each dataset and their associated projection scores depicted on a topographic map are presented in Figure 1. The third eigenfunction, for example, corresponds to a continuous blinking which is characterised by a high energy intensity in the prefrontal area. Physiological non-brain activity that occurs near the recording zone can be easily detected, as they become sources of contrasting amplitude regarding brain activity or other artifacts. In this case, the smoothed KL-FICA presumably attenuates the high-frequency activity associated to brain patterns that interfere in the estimation. Such reasoning can be extended to the first and second artifactual eigenfunctions. Notice that, when the artifact has low-frequency (as the one captured by the first eigenfunction),  $\lambda$  increases considerably whereas other artifactual forms require less smoothing; see Table 1 for more details.

However, when artifacts are characterised by localised high-amplitude curves, as it is the case for the fourth artifactual eigenfunction (chewing), smoothing is not able to mimic those curves and does not discriminate effectively the high-frequency activity produced by other potentials. As has been observed before, this happens because the weight function strongly depends on the noise provided by the fourth-order structure of the model to set up its underlying shape. Thus, these artifacts are quite sensible to smoothing, which in turn can have the opposite effect by causing a loss of accuracy. In addition, we had to increase the range of  $q$  settled to perform KE, leading to the selection among a larger number of eigenfunctions.

**Table 1.** Summary of different parameters and kurtosis of components after performing the P-spline KL-FICA on the different ERP trials. KE is estimated without penalization as well as for the  $\lambda$  obtained with baseline cross-validation (BCV). The shaded kurtosis values of the components are those related to the depicted eigenfunctions in Figure 1.

Trial	$j_0$	$q$	KE	KE	$\lambda_{BCV}$	kurt					
			$\lambda = 0$	$\lambda_{BCV}$	$\zeta_{1,\lambda}$	$\zeta_{2,\lambda}$	$\zeta_{3,\lambda}$	$\zeta_{4,\lambda}$	$\zeta_{5,\lambda}$		
Nodding	6	5	17.80	45.86	4800	48.73	5.473	5.165	3.825	3.601	—
Arm mov.	4	4	4.000	4.518	1000	7.441	2.637	3.736	2.891	—	—
Blinks	4	3	4.128	3.606	300	6.567	3.115	2.476	—	—	—
Chewing	$p$	9	16.52	—	—	16.86	8.326	3.593	9.363	6.170	—

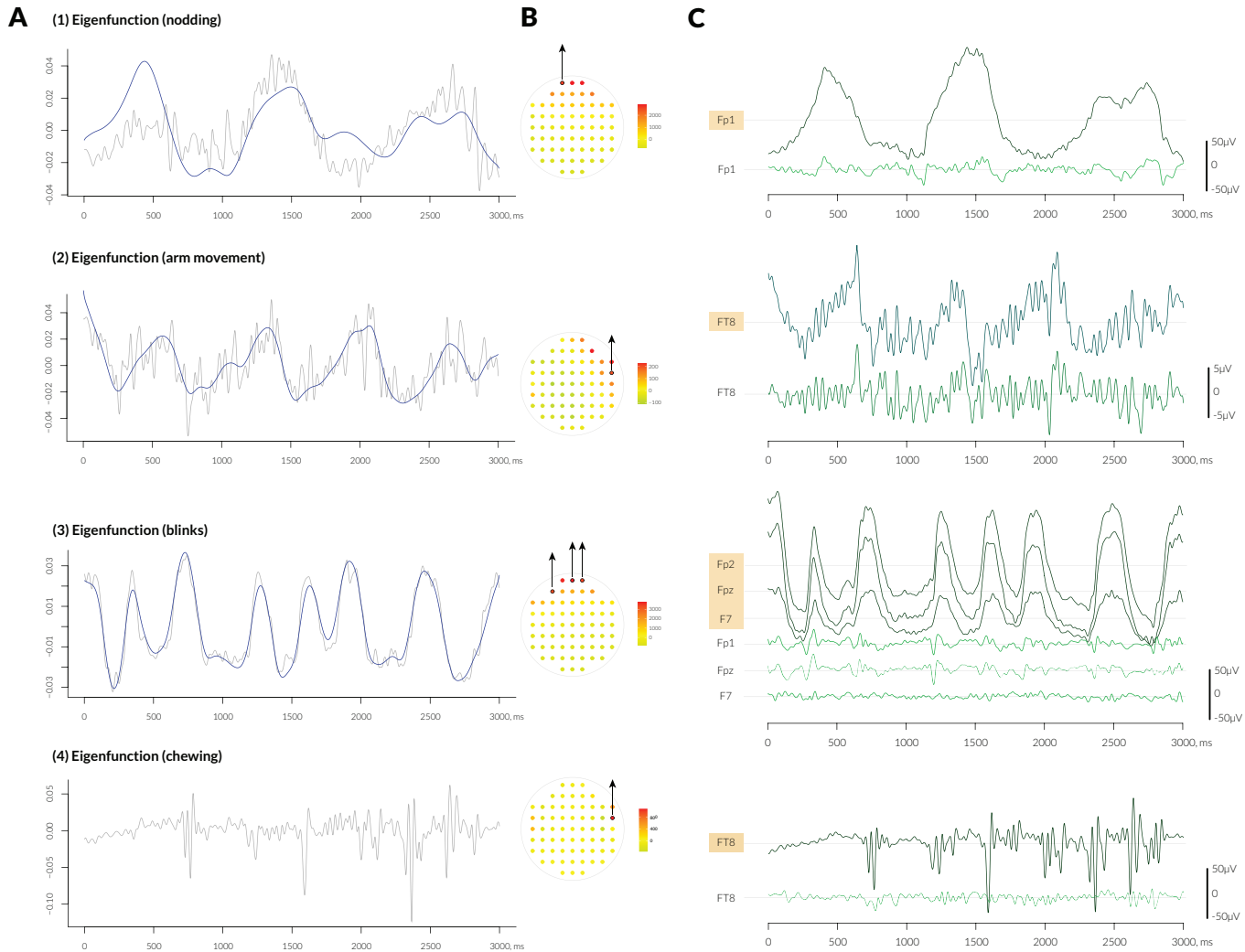


**Figure 1.** (a) A selection of illustrative artifactual eigenfunctions from different single trial ERP data sets using unpenalized KL-FICA (grey) and P-spline KL-FICA (blue) decompositions. The eigenfunctions are ordered from low to high frequency characteristics. (b) The components obtained by projection of the smooth depicted eigenfunction on the original functional sample and distributed in the spatial electrode domain. (c) Comparison of peripheral channels before the extraction, correction and removal (shaded in beige) and after (non-shaded).

From this results it is clearly observed that penalized KL-FICA provides a smooth separation of most common artifacts. We also notice that the second eigenfunction, whose characterisation is of interest for the next section, successfully captures the arm movement in the stipulated time

course. This, however, is only the first half of process to estimate the underlying brain activity. Our tests on such datasets have shown that a good approximation of brain sources can be obtained by subtracting the whole estimated artifactual space. It seems reasonable to conjecture that restricting  $q$  to the first FPCA eigenvalues decreases the odds of obtaining spurious artifactual functions as they represent to higher modes of variability of the FPCA decomposition. Moreover, by having selected an appropriate penalty parameter we may avoid the distortion of the underlying neural activity. Other methods could be considered to fine-tune the selection of artifacts (see [Zima et al., 2012](#)), although their application is not as straightforward for functional data.

### Group-level ERP

To illustrate our method for a group of ERPs, we consider two functional data sets on the following experimental conditions: 1) tap to the sound involving an arm movement, 2) listening without movement, both with  $i = 1, \dots, 64$  and 100 trials per condition. The P-spline KL-FICA is iteratively used to obtain brain estimates by subtracting the smooth artifactual curves in each trial. Here, the complexity of extracting artifacts increases as we now assume a mixture them as well as other brain processes due to the cognitive task. The boxplots of the number of components obtained and the measures of KE by using P-spline KL-FICA for each condition are shown in Figure 3. As we expected, the number of components obtained in condition 1 (movement) is significantly higher than in condition 2 (no movement). In addition, note that KE takes larger values for condition 2; we believe this is a direct consequence of a homogeneous independent mixture of artifactual and cerebral activity.

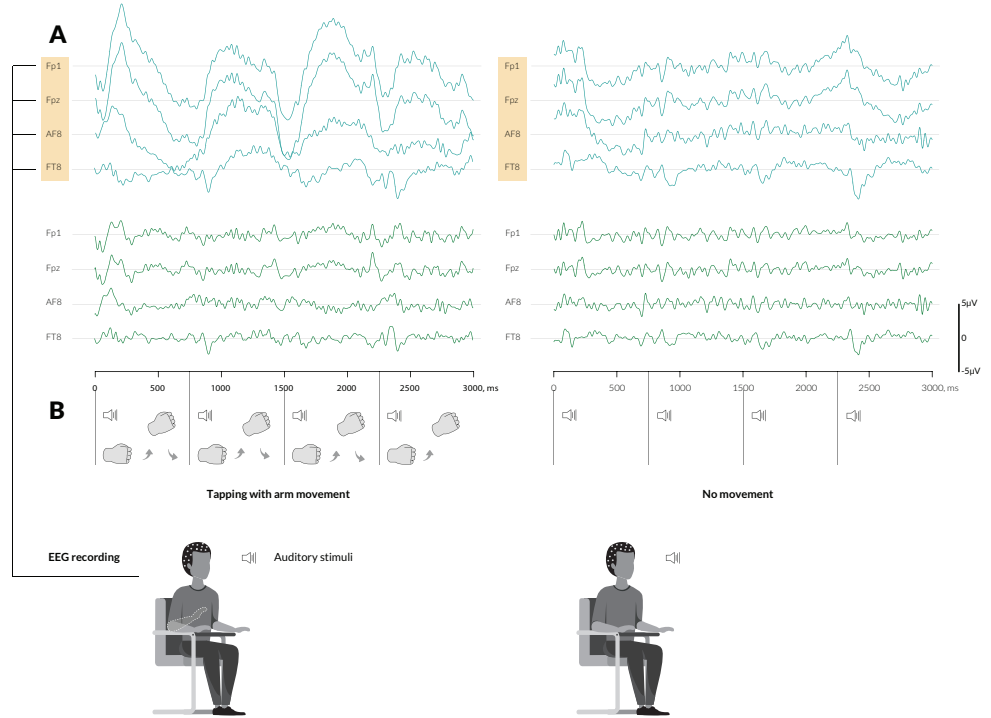


**Figure 2.** (a) Grand average across trials in some prefrontal channels where the artifactual activity is expected. The shaded ones show the raw curves and non-shaded, the curves after artifact removal. (b) A descriptive scheme of the arm movement and corresponding time measures is provided at the bottom of the panels.

Figure 2 shows a contrast between conditions using the proposed approach. All curves from each channel were averaged across trials. The upper left panel displays frontal channels where the movement-related artifact is clearly visible before the subtraction. Further evidence of such artifactual content is given in the right panel where the raw curves in the other condition are shown. Clearly, the accumulated artifacts across the trials have here a different origin. Finally,

the same panel shows the curves after the subtraction of the artifactual curves. We observe that our procedure notably reduces the movement-related artifactual activity and renders the signal more stationary. The same applies to the other condition, although differences are smaller. We show that, in both conditions, our algorithm is still capable of reducing artifactual content while retaining brain activity. However, we may expect some loss of information or distortion (if estimates are oversmoothed) at trial level depending on the selected  $\lambda$ . We also observe that, as the response to the repeated stimulus is assumed to be invariant and small in terms of amplitude, averaging suppresses non-phase-locked activity and reveals the potential elicited by the stimulus (Tong and Thakor, 2009). Consequently, attenuate artifactual sources will lead to a better estimation of brain potentials at averaging rather than subtract rough artifactual curves.

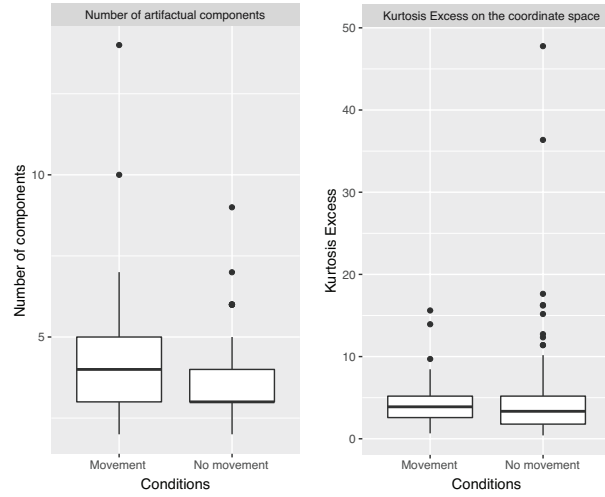


**Figure 3.** Boxplot of the number of components computed using an iterative KL-PFICA on 100 trials per condition and boxplot of related KE measures.

## 6 Concluding remarks

In this paper, we proposed a smoothed FICA approach based on a roughness discrete penalty. The fourth-order blind identification is performed on the smoothed Karhunen-Lo   expansion, extending the functional IC model introduced by Li et al. (2015) in combination with the smooth FPCA proposed by Aguilera and Aguilera-Morillo (2013b) which introduces the P-spline penalty in the orthonormality constraint between principal components. We have shown that conducting the multivariate ICA procedure on the coordinate vectors of the K-L expansion is equivalent to a particular functional ICA of the original B-spline expansions. This equivalence is inherited from the procedure proposed in Oca  a et al. (2007) to compute estimates of functional PCA under general settings, although now, since  $f_j$  are orthogonal the task is simplified. The asymptotic properties of Silverman's method of smooth FPCA has been studied by Lakraj and Ruymgaart (2017) using expansions of the perturbed eigensystem of a smoothed covariance operator, however, there is work to be done ensuring this desirable asymptotic properties on our kurtosis operator.

The goal of this paper was to develop the mathematical framework for identification and removal artifacts from functional EEG data, using smooth estimators to prevent the loss of brain activity. In our tests experiments, the kurtosis operator has proven to work well in capturing artifactual forms with different frequency characteristics. One of the strengths of our model is the double regularisation, providing a more versatile approach which may be beneficial depending on the objectives of preprocessing contaminated EEG data. In essence, the degree of separation is defined through the space dimension, from more dependent (first  $q$  terms of the KL) to more independent, thus  $q$  acts as a regularization parameter in the sense of the PC eigendirections. An

additional penalization using the integrated  $d$ -order derivative might be considered to get more accurate estimations, especially when the obtained IC weight functions are assumed to contain traces of brain activity.

We also introduce some tools to approach  $q$  and  $\lambda$ . The former is selected with the kurtosis distance, a measure that reflects the kurtosis excess in a given coordinate space, the second, with baseline cross validation, a novel approach that does not collapse information for  $p > n$  by taking advantage of shrinkage estimators. To facilitate the identification of artifactual functions, the coordinate vector associated to the IC weight functions of interest was represented in the spatial electrode domain on the scalp. The visual inspection of these topographical maps has reveal interesting insights on the composite spectra of the artifactual curves to determine whether or not might be considered to be subtracted.

In order to provide a more feasible instrument for the researcher, we have proposed a method for artifact removal for a group-level of contaminated functional ERPs. Although our method is quite flexible, it only allows to assemble artifacts with certain characteristics, so it does not enable to gather all the artifactual components in a single space, or at least, functions free of leaked neural activity. However, it is meant as a powerful tool at capturing and denoising low-frequency artifacts related to body movements and other physiological events. In such framework, a discussion is pending on the choice of the regularization parameters as well as the physiological significance of smoothing. We observed that, in the trials where the subject was performing a motor and perceptual task, the values obtained by baseline cross-validation were more variable than in our tests. This is probably in part due to a more complex mixture of brain and artifactual activity. Despite our choice was to exploit the minimization of BCV, clearly there are other possible approaches to consider. We see that our method paves the way to further developments in the field of neural signal processing: in the future a review for performance comparison with different FOBI estimators and extensions of other ICA methodologies would be interesting as well.

## 7 Software

P-spline KL-FICA was conducted using a modified version of `pspline.ffaobi` function of the `pfica` R package (Vidal and Aguilera, 2020). The implemented code together with a sample input data sets and documentation are available on request from the corresponding author (M.V.).

## Author Contributions

**Marc Vidal:** Conceptualization, Methodology, Software, Data collection, Writing – original draft. **Mattia Rosso:** Experimental design, Data collection, Preprocessing, Writing – editing. **Ana M. Aguilera:** Methodology, Writing – review and editing, Supervision.

## Acknowledgments

We thank Daniel Gost for helping with figures and formatting. The research of Marc Vidal was supported by the Methusalem funding from the Flemish Government given to Marc Leman. The authors thank the support of the Spanish Ministry of Science, Innovation and Universities under project MTM2017-88708-P also supported by the FEDER program) and research group FQM307 funded by the Government of Andalusia (Spain).

*Conflict of Interest:* None declared.

## References

Aguilera AM, Aguilera-Morillo MC. Comparative study of different B-spline approaches for functional data. Mathematical and Computer Modelling. 2013; 58:1568–1579.

Aguilera AM, Aguilera-Morillo MC. Penalized PCA approaches for B-spline expansions of smooth functional data. Applied Mathematics and Computation. 2013; 219:7805–7819.

**Akhtar MT**, Mitsuhashi W, James CJ. Employing spatially constrained ICA and wavelet denoising, for automatic removal of artifacts from multichannel EEG data. *Signal Processing*. 2012; 92:401–416.

**Ash RB**, Gardner MF. Topics in stochastic processes. New York: Academic Press; 1975.

**Bell AJ**, Sejnowski TJ. An information-maximization approach to blind separation and blind deconvolution. *Neural Computation*. 1995; 7:1129–1159.

**Buzsáki G**. Rhythms of the Brain. Oxford University Press; 2006.

**Cardoso JF**. Source separation using higher order moments. In: *Proceedings of IEEE international conference on acoustics, speech and signal processing*; 1989. p. 2109–2112.

**Cardoso JF**, Souloumiac A. Blind beamforming for non-Gaussian signals. In: *IEE Proceedings F-Radar and Signal Processing*, vol. 140; 1993. p. 362–370.

**Castellanos NP**, Makarov VA. Recovering EEG brain signals: Artifact suppression with wavelet enhanced independent component analysis. *Journal of Neuroscience Methods*. 2006; 158:300 – 312.

**Eilers PHC**, Marx BD. Flexible smoothing with b-splines and penalties. *Statistical Science*. 1996; 11:89–121.

**Ghanem R**, Spanos P. Stochastic Finite Elements: A Spectral Approach. New York: Springer-Verlag; 1991.

**Gramann K**, An introduction to mobile brain/body imaging (MoBI); 2014.

**Gutch H**, Theis F. To infinity and beyond: On ICA over Hilbert spaces. In: Theis F, Cichocki A, Yeredor A, Zibulevsky M, editors. *Latent Variable Analysis and Signal Separation*; 2012. p. 180–187.

**Hasenstab K**, Scheffler A, Telesca D, Sugar CA, Jeste S, DiStefano C, Sentürk D. A multi-dimensional functional principal components analysis of EEG data. *Biometrics*. 2017; 3(73):999–1009.

**Herault J**, Jutten C. Space or time adaptive signal processing by neural models. In: Denker JS, editor. *AIP Conference: Neural Networks for Computing*, vol. 151 American Institute for Physics; 1986. p. 206–211.

**Hyvärinen A**, Oja E. A fast fixed-point algorithm for independent component analysis. *Neural Computation*. 1997; 9:1483–1492.

**Kelly JW**, Siewiorek DP, Smailagic A, Collinger JL, Weber DJ, Wang W. Fully automated reduction of ocular artifacts in high-dimensional neural data. *IEEE Transactions on Biomedical Engineering*. 2011; 58:598–606.

**Kollo T**. Multivariate skewness and kurtosis measures with an application in ICA. *Journal of Multivariate Analysis*. 2008; 99(10):2328–2338.

**Lakraj GP**, Ruymgaart F. Some asymptotic theory for Silverman's smoothed functional principal components in an abstract Hilbert space. *Journal of Multivariate Analysise*. 2017; 155:122–132.

**Li B**, Bever GV, Oja H, Sabolová R, Critchley F. Functional independent component analysis: an extension of the fourth-orderblind identification.; 2015, submitted.

**Loperfido N**. A new kurtosis matrix, with statistical applications. *Linear Algebra and its Applications*. 2017; 512:1–17.

**Mahajan R**, Morshed BI. Unsupervised eye blink artifact denoising of EEG data with modified multiscale sample entropy, kurtosis, and Wavelet-ICA. *IEEE Journal of Biomedical and Health Informatics*. 2015; 19:158–165.

**Muthukumaraswamy SD**. High-frequency brain activity and muscle artifacts in MEG/EEG: a review and recommendations. *Frontiers in human neuroscience*. 2013; 7:138.

**Nie Y**, Wang L, Liu B, Cao J. Supervised functional principal component analysis. *Statistics and Computing*. 2018; 28:713–723.

**Nordhausen K**, Virta J. An overview of properties and extensions of FOBI. *Knowledge-Based Systems*. 2019; 173:113–116.

**Nunez PL**, Srinivasan R. Electric fields of the brain: the neurophysics of EEG. Oxford: Oxford University Press; 2006.

**Ocaña FA**, Aguilera AM, Escabias M. Computational considerations in functional principal component analysis. *Computational Statistics*. 2007; 22:449–465.

**Peña C**, Prieto J, Rendón C. Independent components techniques based on kurtosis for functional data analysis. Universidad Carlos III de Madrid; 2014.

**Pokora O**, Kolacek J, Chiu T, Qiu W. Functional data analysis of single-trial auditory evoked potentials recorded in the awake rat. *Biosystems*. 2018; 161:67–75.

**Ramsay J**, Silverman BW. Functional Data Analysis. New York: Springer; 2005.

**Rice JA**, Silverman BW. Estimating the Mean and Covariance Structure Nonparametrically When the Data are Curves. *Journal of the Royal Statistical Society: Series B (Methodological)*. 1991; 53(1):233–243.

**Schäfer J**, Strimmer K. A shrinkage approach to large-scale covariance matrix estimation and implications for functional genomics. *Statistical Applications in Genetics and Molecular Biology*. 2005; 4:1–29.

**Scheffler A**, Telesca D, Q Li Q, Sugar CA, Distefano C, Jeste S, Şentürk D. Hybrid principal components analysis for region-referenced longitudinal functional EEG data. *Biostatistics*. 2018; 21:139–157.

**Silverman BW**. Smoothed functional principal components analysis by choice of norm. *The Annals of Statistics*. 1996; 24:1–24.

**Singh YN**, Singh SK, Ray AK. Bioelectrical signals as emerging biometrics: Issues and challenges. *ISRN signal processing*. 2012; 2012:1–13.

**Tian TS**. Functional data analysis in brain imaging studies. *Frontiers Psychology*. 2010; 1:1–11.

**Tong S**, Thakor NV. In: *Quantitative EEG analysis methods and clinical applications*; 2009. .

**Vidal M**, Aguilera AM. pfica: Penalized Independent Component Analysis for Univariate Functional Data; 2020, <https://CRAN.R-project.org/package=pfica>, r package version 0.1.1.

**Virta J**, Li B, Nordhausen K, Oja H. Independent component analysis for multivariate functional data. *Journal of Multivariate Analysis*. 2020; 176:1–19.

**Wang X**. Neurophysiological and computational principles of cortical rhythms in cognition. *Physiological reviews*. 2010; 90:1195–1268.

**Xiao L**. Asymptotic theory of penalized splines. *Electronic Journal of Statistics*. 2019; 13:747–794.

**Yao F**, Müller HG, Wang JL. Functional Data Analysis for Sparse Longitudinal Data. *Journal of the American Statistical Association*. 2005; 100(470):577–590.

**Zima M**, Tichavský P, Paul K, Krajča V. Robust removal of short-duration artifacts in long neonatal EEG recordings using wavelet-enhanced ICA and adaptive combining of tentative reconstructions. *Physiological Measurement*. 2012; 33:39 – 49.